Available online at www.sciencedirect.com
SCIENCE DIRECT
Polymer 46 (2005) 775–783
polymer
www.elsevier.com/locate/polymer

Polyurethane/clay nanocomposites foams: processing, structure and properties

Xia Cao[a], L. James Lee[a,*], Tomy Widya[b], Christopher Macosko[b]

[a]Department of Chemical and Biomolecular Engineering, The Ohio State University, Columbus, OH 43210, USA
[b]Department of Chemical Engineering, University of Minnesota, Minneapolis, MN, USA

Received 19 August 2004; received in revised form 3 November 2004; accepted 17 November 2004
Available online 8 December 2004

Abstract

Polyurethane (PU)/montmorillonite (MMT) nanocomposites were synthesized with organically modified layered silicates (organoclays) by in situ polymerization and foams were prepared by a batch process. Clay dispersion of polyurethane nanocomposites was investigated by X-ray diffraction and transmission electron microscopy. The morphology and properties of PU nanocomposites and foams greatly depend on the functional groups of the organic modifiers, synthesis procedure, and molecular weight of polyols because of the chemical reactions and physical interactions involved. Silicate layers of organoclay can be exfoliated in the PU matrix by adding hydroxyl and organotin functional groups on the clay surface. The presence of clay results in an increase in cell density and a reduction of cell size compared to pure PU foam. In the polyurethane with high molecular weight polyol, a 6 °C increase in T_g, 650% increase in reduced compressive strength, and 780% increase in reduced modulus were observed with the addition of 5% organically treated clays. Opposite effects were observed in PU nanocomposite foams with highly crosslinked structure. The interference of the H-bond in the presence of clay is probably the reason.

Keywords: Polyurethane (PU); Organoclay; Clay dispersion

1. Introduction

Polymer-layered silicate nanocomposites have recently gained a great deal of attention because they offer a great potential to provide superior properties when compared to pure polymers and conventional filled composites. The properties include high dimensional stability, high heat deflection temperature, reduced gas permeability, improved flame retardance, and enhanced mechanical properties [1–3]. Since the advent of nylon-6/montomorillonite nanocomposites developed by Toyota Motor Co., the studies on polymer/clay nanocomposites have been successfully extended to many other polymer systems [2].

Polyurethanes (PUs) are unique polymer materials with a wide range of physical and chemical properties. With well-designed combinations of monomeric materials, PUs can be tailored to meet diversified demands of various applications such as coatings, adhesives, fibers, thermoplastic elastomers, and foams. However, PUs also have some disadvantages, such as low thermal stability and low mechanical strength, etc. To overcome these disadvantages, a great deal of effort has been devoted to the development of nanostructured polyurethane (PU)/montmorillonite (MMT) composites in recent years [4–7].

The effects of clay type, clay content, and PU molecular structure on clay dispersion in thermoplastic PU nanocomposites have been studied. It has been found that MMT clays exchanged with long chain oniumions (carbon number > 12) have good compatibility with polyol. The extent of gallery expansion of modified MMT is mainly determined by the chain length of the gallery oniumions [4]. A good dispersion of layered silicate has been found to improve the properties of PU elastomer nanocomposites, such as mechanical properties, thermal stability and gas permeability [5–7]. Good dispersion of clays in the PU matrix has been achieved through the modification of MMT with active surfactants containing more than two hydroxyl

* Corresponding author. Tel.: +1 614 292 2408; fax: +1 614 292 3769.
E-mail address: lee.31@osu.edu (L. James Lee).

0032-3861/$ - see front matter © 2004 Published by Elsevier Ltd.
doi:10.1016/j.polymer.2004.11.028

groups [6]. The presence of hydroxyl groups enhanced intra-gallery polymerization, which in turn led to better clay dispersion. However, the morphology of nanocomposites prepared by this approach was still a combination of exfoliation/intercalation and the method only worked at low clay content, i.e. less than 3 wt%, even for organoclay modified by surfactants with three hydroxyl groups. The exfoliated clay dispersion was only observed at low reaction rates in solution polymerization [6].

Polyurethane (PU) foams account for the largest market among polymeric foams, estimated at nearly two billion kilograms in the US alone [8]. PU foams have a remarkably broad range of applications including thermal insulation, cushioning, buoyancy, energy absorption (packaging), etc. Their low density also permits the design of light, stiff components such as aircraft-interior panels, structural shapes (transom cores, bulkhead core, stringers, motor-mounts, etc.) in fiber-reinforced plastic (FRP) boat building, impact-limiters and crash-pads, composite foam cores, mold-patterns and plugs, sports-equipment core material, and composite tooling. Mechanical properties are important considerations for such structural and semi-structural applications. Unlike thermoplastic foams, PU foams are formed by reactive processing, in which polymerization and foam blowing occur simultaneously. Polymer structure must build up rapidly to support the fragile foam, but not too fast to stop bubble growth.

For thermoplastic foams, it was found that clay-filled nanocomposites could effectively reduce the cell size and increase the cell density [9,10]. An exfoliated PS nanocomposite produced a foam with a cell size five times smaller than that of the pure PS foam [9]. Several advantages can be expected in using a PU nanocomposite as the matrix of PU foams. The presence of nanoparticles may improve the mechanical strength of the PU matrix and in turn the strength of the PU foam. Nanoscale-dispersed clay may act as nucleation agents during the foaming process to produce finer cell structure and higher cell density. Furthermore, improved gas barrier properties [5] provide another opportunity for application of nanoclay in PU foams.

Currently there are very few studies in the literature regarding the use of nanoclay in the reactive PU foaming process. Only one published patent has demonstrated that nanoclay improved the thermal insulation and aging properties of PU foam (indicated by *k*-factors in Btu.in/ft^2.h.F). The polyurethane foam was made both without and with up to 10 wt% Cloisite 10A. The foam without nanoclay gave initial and aged *k*-factors of 0.139 and 0.193, while the foam with nanoclay gave initial and aged *k*-factors of 0.135 and 0.182 [11]. A better understanding is needed on effect of the clay dispersion on foaming processes and structure/property relationships. In this study, PU nanocomposites as well as their foams were prepared by in situ polymerization and batch foaming with different modified MMTs. The effects of surface modification of the clay, polyol molecular weight, and the route of PU/clay synthesis were investigated. The morphology of nanocomposites was characterized by X-ray diffraction (XRD) and transmission electron microscopy (TEM). The influence of modified nanoclays on the cell structure and properties of PU nanocomposite foams was also studied.

2. Experimental

2.1. Materials

The commercial nanoclay used in this study was provided by Southern Clay Products, Cloisite® 30B (MMT-OH), a montmorillonite modified by methyl tallow bis-2-hydroxyethyl ammonium with a concentration of 90 meq/100 g clay. Dibutyldimethoxytin (DBDMT, Aldrich Chemicals) was also used to modify Cloisite® 30B to provide inter-gallery analytic function during the polyurethane reaction.

The isocyanate used in this study was a polymeric aromatic isocyanate based on diphenylmethane 4, 4′-diisocyanate (MDI) from Bayer Group, Mondur MRS-4 (NCO index: 129; functionality: 2.4; viscosity at 25 °C: 40 MPa). Two tri-functional polyester polyols from Dow Chemical, Tone 0305 (OH value: 311.5; Mn: 540, viscosity at 55 °C: 200 MPa) and TONE 0301 (OH value: 561.5; Mn: 300, viscosity at 55 °C: 230 MPa) were used in this study. DABCO T-12 from Air Products and Chemicals was used as the catalyst. A mixture of cyclopentane and isopentane at 70:30 by weight was used as the blowing agent. TEGOSTAB B8462 from Degussa/Goldschmidt Chemical Corp. was used as the surfactant to prepare PU foams.

2.2. Preparation of organoclay with catalytic function

Cloisite® 30B was modified by DBDMT. The hydroxyl groups on the surface modifier of 30B were converted into stannous alkoxides at 50 °C for 4 h through the reaction with DBDMT in toluene at 5% clay content. The surface-treated clay was then filtered using a Busch filter and redispersed in toluene. This procedure was repeated five times to remove the residual surface modifier. The product was then placed in a vacuum oven at 100 °C for 12 h. The dried product was ground into fine powder to obtain organophilic montmorillonite with catalytic function, denoted as MMT-Tin.

2.3. Synthesis of PU nanocomposites and foams

MDI and polyols were dehydrated under vacuum overnight at room temperature and 60 °C, respectively. All clays were dehydrated in an oven at 100 °C overnight before use. For PU nanocomposites, clay was first mixed with one monomer by a high shear mixer for 2 min, and then mixed for another 30 s after the other monomer was added.

Catalyst was always added with polyol. Polymerization was carried out at ambient condition. The prepared hybrid was then post-cured in an oven at 100 °C for 4 h. Excess MDI (ca. 5 mol%; NCO/OH) was used to assure the complete reaction of polyol.

For reactive foaming of PU, TEGOSTAB B8462 was used as the surfactant at 0.66 wt% and pentane as the blowing agent at 5.5 wt%. Pentanes were placed in a refrigerator at 0 °C before use to reduce evaporation during sample preparation. The mixture of all ingredients was mixed by an impeller at 2000 rpm and foaming occurred in a closed plastic container with fixed volume at ambient temperature. The foams were then transferred into an oven at 100 °C for 4 h to ensure completion of the reaction.

2.4. Measurements and characterization

The thermal stability of the organic species on the organoclay was determined by Thermogravimetric Analysis (TGA, Perkin-Elmer TGA 7) under a nitrogen atmosphere. The sample was heated from room temperature to 840 °C at 20 °C/min.

Rheological measurement of either polyol or isocyanate with dispersed organoclays was carried out using a stress-controlled rheometer (Physica™ MCR300). A temperature controller with a Peltier element was employed to maintain a constant temperature during testing. The diameter of the parallel plates was 50 mm, and the gap between them was about 1 mm. Viscosity was measured under isothermal condition (25 °C) and at a shear rate sweep from 0.1 to 100 s^{-1}.

The clay dispersion was determined by XRD on a Scintag XDS-2000 X-ray diffractometer equipped with an intrinsic germanium detector system using Cu Kα radiation ($\lambda = 1.5418$ Å). Transmission electron microscopy (TEM) was also adopted to characterize the nanocomposite structure. TEM was performed on a Phillip CM12 using an accelerating voltage of 80 kV. The nanocomposites were sectioned into ultra-thin slices (<100 nm) at room temperature using a microtome and then mounted on 200 mesh copper grids.

The glass transition temperatures (T_g) of neat PU and PU nanocomposite foams were determined by using a thermo-mechanical analyzer (TMA 2940, TA Instruments), operated at a heating rate of 5 °C/min with 0.01 N preloaded force.

The cellular morphologies of the foamed samples in the rising direction were investigated by a Philips XL30 scanning electron microscope (SEM). Samples were freeze-fractured in liquid nitrogen and the fracture surface was sputter-coated with gold before observation. Image analysis was performed on the SEM micrographs using Scion Image software (Scion Corporation) to obtain the average cell size and cell density [9]. The bulk density of the foams was estimated by directly measuring the weight and volume of the cubic foam samples.

The compressive strength and modulus parallel to the rising direction of foam samples were measured by an INSTRON® 5848 Microtester according to ASTM D1621. The specimens had dimensions of $25.4 \times 25.4 \times 12.7$ mm^3 and the crosshead speed of compression was set at 1.2 mm/min.

3. Results and discussion

3.1. Characterization of clays

In this study, MMT-OH was modified by DBDMT ($((CH_3CH_2CH_2CH_2)_2Sn(OCH_3)_2$), an effective catalyst for polyurethane reaction. The modification was carried out by the alkoxide-alcohol exchange as described in Scheme 1 to prepare organoclays with catalytic function, MMT-Tin [12].

To determine the content of the catalytic component in the modified clay, MMT-Tin, a TGA test was carried out in a nitrogen atmosphere from room temperature to 840 °C at 20 °C/min. The exchanged portion in the inter-galleries of silicates was determined by the weight residue difference between the MMT-OH and MMT-Tin in the temperature range from 120 to 800 °C in TGA [6]. Fig. 1 shows that both MMT-OH and MMT-Tin experienced larger weight loss compared to MMT, and the weight loss of MMT-Tin is 1.1% more than that of MMT-OH. This indicates that the organic component on the clay surface increases after surface treatment by DBDMT. According to Scheme 1, the concentration of stannous alkoxides in MMT-Tin is 4.17 meq/100 g clay. The exchange efficiency could be improved by distilling off the azeotropic mixture formed by toluene with the released methanol and shifting the alcohol/alkoxide equilibrium completely towards the right side of Scheme 1 [12].

XRD patterns of the raw clay and organoclays are shown in Fig. 2. The basal spacing of the organoclay increased compared to MMT ($d_{001} = 1.16$ nm) because the gallery of MMT was expanded by molecular chains of the surface modifier. However, the d-spacing decreased from 1.77 to 1.43 nm when MMT-OH was further modified by DBDMT. There are two methoxy groups on every DBDMT. They could conjugate with each other on the clay layer through alkoxide-alcohol exchange. A DBDMT bridge between two clay layers may form if hydroxyl groups are from different layers. This could result in a smaller gallery spacing even though the organic content in MMT-Tin is slightly higher than in MMT-OH.

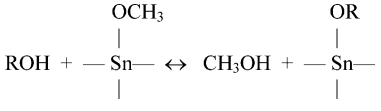

Scheme 1.

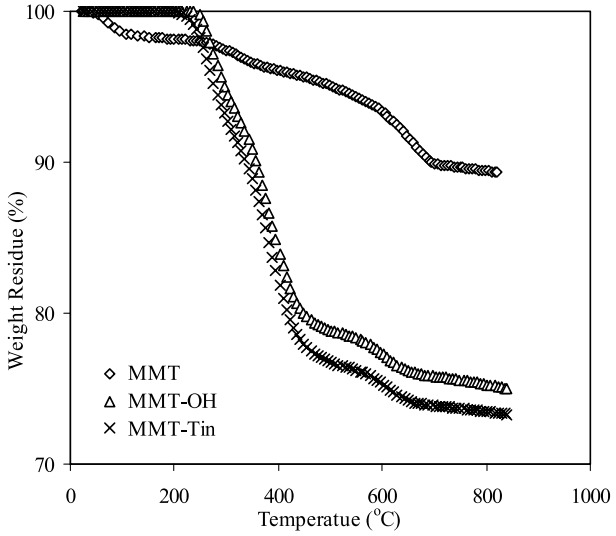

Fig. 1. Thermogravimetric analysis curves (20 °C/min) for surface treated MMT.

3.2. PU Nanocomposites

To study the effect of the clay-monomer mixing sequence on clay dispersion, 5% MMT-OH was premixed with either polyol (Tone 0305) or isocyanate (MRS-4) before adding the other monomer. For comparison, PU nanocomposites were also prepared by mixing all ingredients simultaneously. As shown in Fig. 3, the nanocomposite prepared by the one-step approach shows a clear peak at $2\theta = 2.6°$, which indicates a d_{001} spacing shifting from 1.77 to 3.37 nm. This confirmed that polyurethane chains diffused into the gallery of MMT-OH, causing intercalation. The two-step processes offered better clay dispersion than the one-step approach. A shoulder at $2\theta = 2.6°$ on the XRD

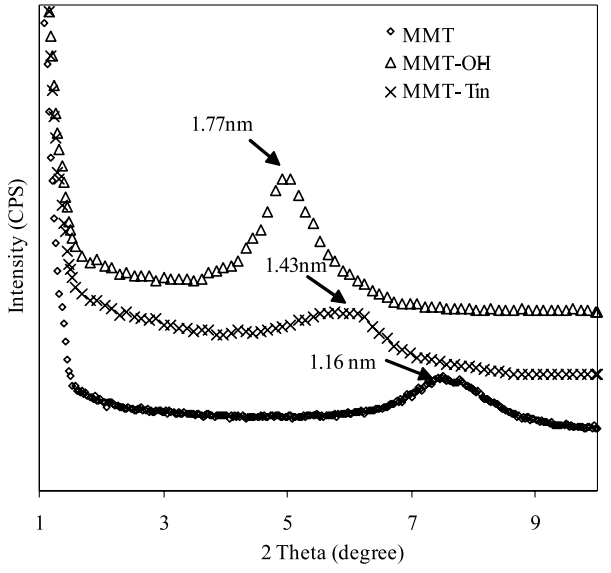

Fig. 2. XRD curves of organoclays with different functional groups (scan at 1°/min).

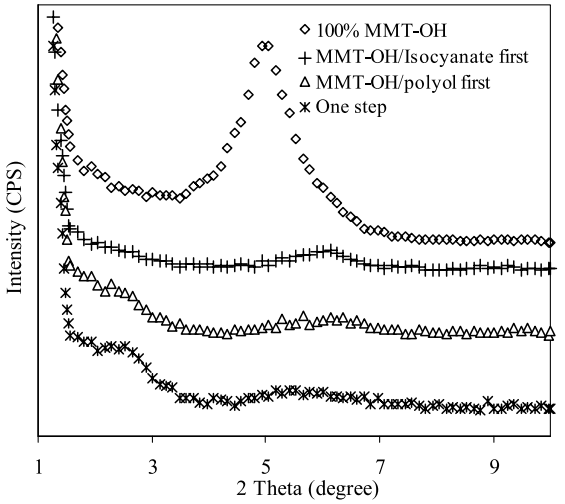

Fig. 3. XRD of 5% MMT-OH/PU nanocomposites prepared by different mixing procedures (polyol: Tone 0305).

curve appeared when MMT-OH was premixed with polyol first. This shoulder completely disappeared when the clay was first mixed with isocyanate. This difference is a result of the reaction between the isocyanate monomers and the hydroxyl groups on alkyl chains of MMT-OH, which is demonstrated by the FTIR spectra change in Fig. 4. The absorption peak of isocyanate at 2278 cm^{-1} could be followed for kinetics study during the reaction [13]. Fig. 4 shows that the peak area at 2278 cm^{-1} decreased with time after the isocyanate monomer was mixed with MMT-OH, indicating a reaction between isocyanate and hydroxyl groups on the clay surface. This caused an increase of gallery spacing of clay to facilitate clay exfoliation. The shear viscosity of MMT-OH/polyol and MMT-OH/isocyanate suspension at the same MMT-OH content was also measured at 25 °C. Since a large viscosity difference exists between isocyanate and polyol, a relative viscosity was used to compare the viscosity change due to the presence of clay

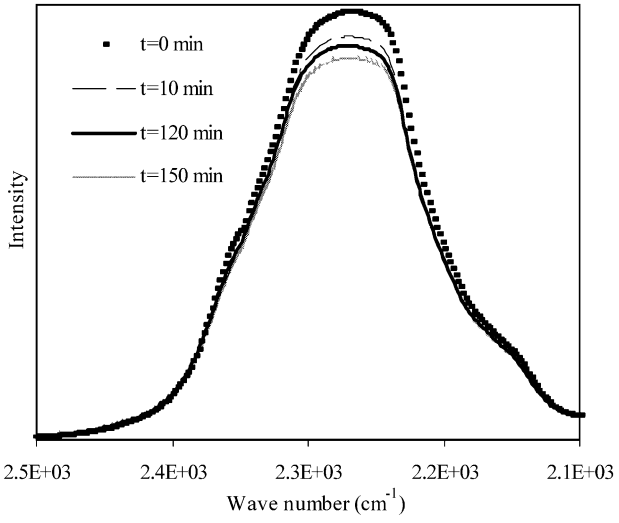

Fig. 4. FTIR spectra of isocyanate and MMT-OH at different times.

in monomer. The relative viscosity is defined as the viscosity of the clay suspension divided by the viscosity of the solvent, in this case, either isocyanate or polyol. The clay content was fixed at 10 wt%. It can be clearly seen from Fig. 5 that the relative viscosity of the MMT-OH/isocyanate suspension is higher than that of the MMT-OH/polyol suspension, and the presence of a catalyst (i.e. MMT-Tin) further increases the viscosity. This provides further evidence of better clay dispersion in isocyanate because of the reaction between isocyanate and hydroxyl groups on the clay surface. This 'organoclay/isocyanate first' mixing sequence was used to prepare PU nanocomposites and foams in the remaining studies.

The XRD spectra of PU/clay (5 wt%) hybrids with clays bearing different surface functional groups are shown in Fig. 6(a). It can be seen that no diffraction peak was observed for PU nanocomposites with MMT-Tin and its XRD pattern is very close to that of the pristine PU. More detailed clay dispersion is shown by TEM images in Fig. 7. Nanocomposites containing both MMT-OH and MMT-Tin reveal good clay dispersion with MMT-Tin showing better exfoliation. A small amount of stacking of clay layers with substantial layer separation is visible (marked in circles Fig. 7(a) and (b)). As seen from the TEM images at low magnification, the overall clay distribution of MMT-Tin in the PU hybrid is more uniform than MMT-OH. Better dispersion of MMT-Tin may result from the intra-gallery catalysis of organotin.

3.3. PU Nanocomposite foams

Reactive foaming of PU nanocomposites containing clays with different functionalities was carried out at ambient temperature. The clay content was fixed at 5% based on the overall weight of PU, and the gel time was

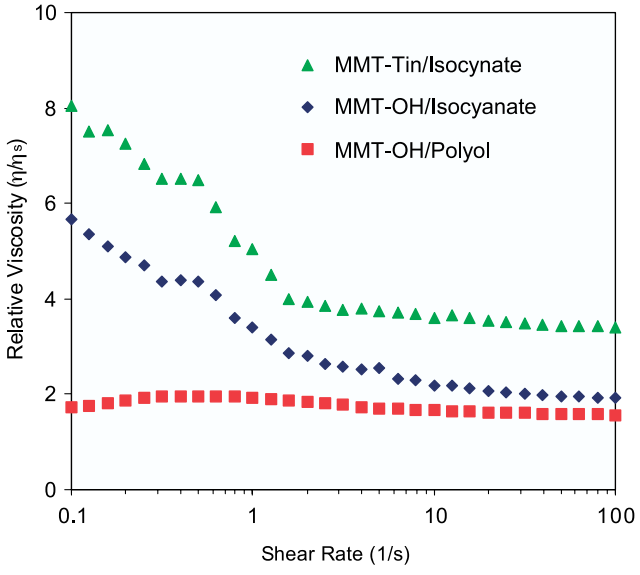

Fig. 5. Relative viscosity of organoclay/polyol and organoclay/isocyanate suspensions (polyol: Tone 0305).

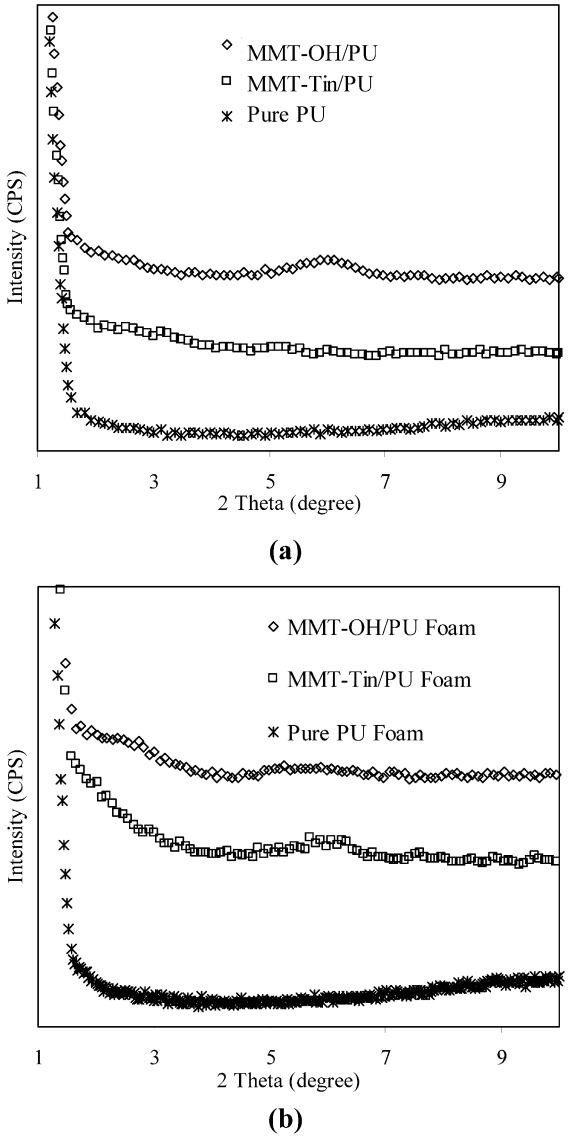

Fig. 6. XRD curves of 5 wt% clay/PU (a) nanocomposites and (b) foams (polyol: Tone 0305).

adjusted to nearly 30 s for all systems by adding different amounts of DABCO T-12. Fig. 8 shows SEM images of the freeze-fractured surface of PU foams. All foams exhibit polygon closed-cell structures with energetically-stable pentagonal and hexagonal faces. The neat PU foam has fewer cells and a larger cell size than PU nanocomposite foams with 5% organoclay. From SEM images, the cell size and density were measured and summarized in Table 1. PU

Table 1
Cell morphology of PU foams (polyol: Tone 0305)

Foam	ρ_f (kg m^{-3})	D (mm)	$N_c \times 10^{-5}$ (cells/cm^{-3})
No clay	77±10	0.26±0.1	0.50
MMT-OH/PU	65±3	0.20±0.08	1.05
MMT-Tin/PU	58±3	0.21±0.06	0.92

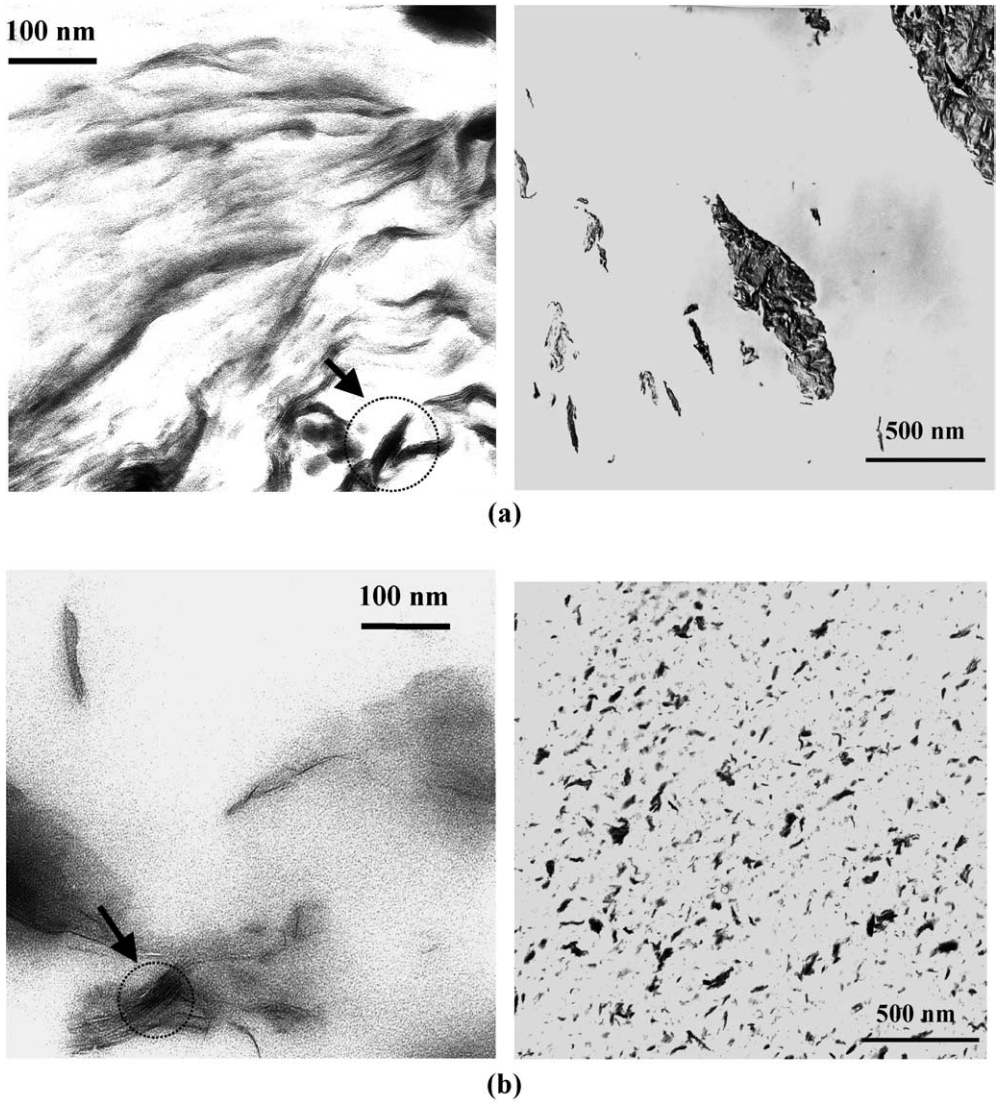

Fig. 7. Transmission electron micrographs of cross-section views of PU nanocomposites (polyol: Tone 0305): (a) 5% MMT-OH/PU b) 5% MMT-Tin/PU.

foams containing 5% organoclays have a lower bulk density (ρ_f) than that of pure PU foam but a higher cell density (N_c) and smaller cell size (d), suggesting that the dispersed clay particles act as heterogeneous nucleation sites during cell formation [14,15]. However, there is little difference between MMT-Tin/PU and MMT-OH/PU nanocomposite foams in terms of cell size and cell density. PU nanocomposite foams were crushed into fine powder and then the clay dispersion was determined by XRD spectra of the powder. Fig. 6(b) shows that diffraction peaks were also absent in the foamed samples, but a shoulder was observed at very low angle. This implies that clay orientation and dispersion is somewhat affected by the foaming process. The shoulder at a very low angle of the XRD pattern of the MMT-Tin/PU foam is smaller than that of MMT-OH/PU foam. The detailed mechanism on how nanoparticles influence cell morphology needs further investigation.

3.4. Properties of PU nanocomposite foams

To study the effect of surface functionality of the nanoclay on physical and mechanical properties, a series of PU nanocomposite foams were prepared. Two model PU systems were chosen in this study. Both of them are polyester triol-based PUs with crosslinked structure varied by the molecular weight of the triols. The lower molecular weight Tone 0301 provides a more rigid foam that that of Tone 0305. The compressive properties and glass transition temperature of the foams were measured.

To exclude the density difference of the foam samples, the reduced compressive strength and modulus (i.e. compressive strength and modulus divided by the density of the foam sample) were used to compare the mechanical properties of the PU foams with different clays. The properties of the PU foams prepared by Tone 0305 are summarized in Fig. 9. As shown in Fig. 9(a), the

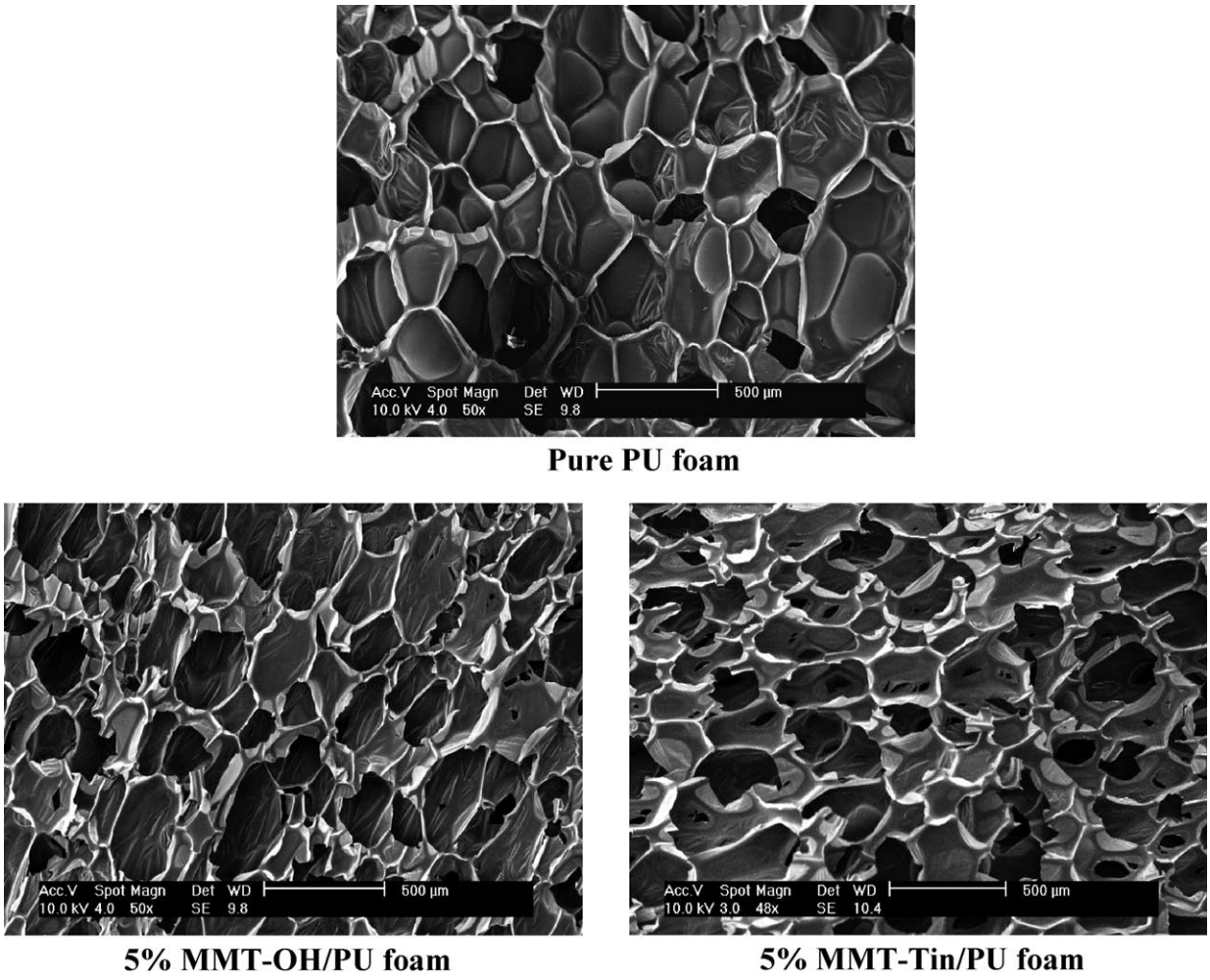

Fig. 8. SEM Micrographs of PU foams at cross-sections parallel to foam rising direction (polyol: Tone 0305).

nanocomposite foams exhibit a substantially higher reduced compressive strength and modulus. Compared to the pure polyurethane foam, the MMT-OH/PU nanocomposite foam shows about a 650% increase in reduced strength and a 780% increase in reduced modulus, while the nanocomposite foam with MMT-Tin shows about a 610% increase in reduced strength and a 760% increase in reduced modulus. The glass transition temperatures of foams shown in Fig. 9(b) indicate that the MMT-Tin/PU foam has the highest T_g, which is 6 and 2 °C higher than that of neat PU and MMT-OH/PU foams, respectively. The higher T_g of PU nanocomposite foams may result from the confinement of PU molecules by dispersed MMT particles. This effect is stronger in the MMT-Tin/PU foam since the catalytic organotin could enhance the intra-gallery reaction.

When PU foams were prepared by a triol with lower molecular weight, i.e. TONE 0301, the presence of nanoclays shows an opposite effect on the properties as compared to the less rigid PU foams. The compressive properties are summarized in Fig. 10(a). Compared to the neat PU foam, the MMT-OH/PU foam has a lower bulk density (62 kg/m^3 vs. 68 kg/m^3). It shows a 7% decrease of the reduced strength from 8.4 to 7.8 MPa/(g/cm^3) and a 39% decrease of the reduced modulus from 192 to 117 MPa/(g/cm^3). The MMT-Tin/PU foam suffers even more in compressive properties. It has about a 2% weight reduction compared to the pure PU foam (67 kg/m^3 vs. 68 kg/m^3) but a 44% decrease of reduced strength from 8.4 to 4.8 MPa/(g/cm^3) and a 55% decrease of modulus from 192 to 90 MPa/(g/cm^3). The glass transition temperatures of PU nanocomposite foams are also lower than that of pristine PU foam as shown in Fig. 10(b). Again, MMT-Tin/PU foam suffers the most and the glass transition temperature is about 8 °C lower than neat PU foam.

It is well known that H-bond formation among urethane groups greatly contributes to the strength and modulus of PUs. For the organoclays used in this study, the PU molecules can be grafted onto the clay surface through the reaction between the –NCO groups and the –OH groups on the clay. The tethered clay may interfere with the H-bond formation in PU as shown in Fig. 11, causing a negative effect on the properties of PU nanocomposite foams. Furthermore, the involvement of organoclays in the reaction could also affect the network structure formation of PU. For

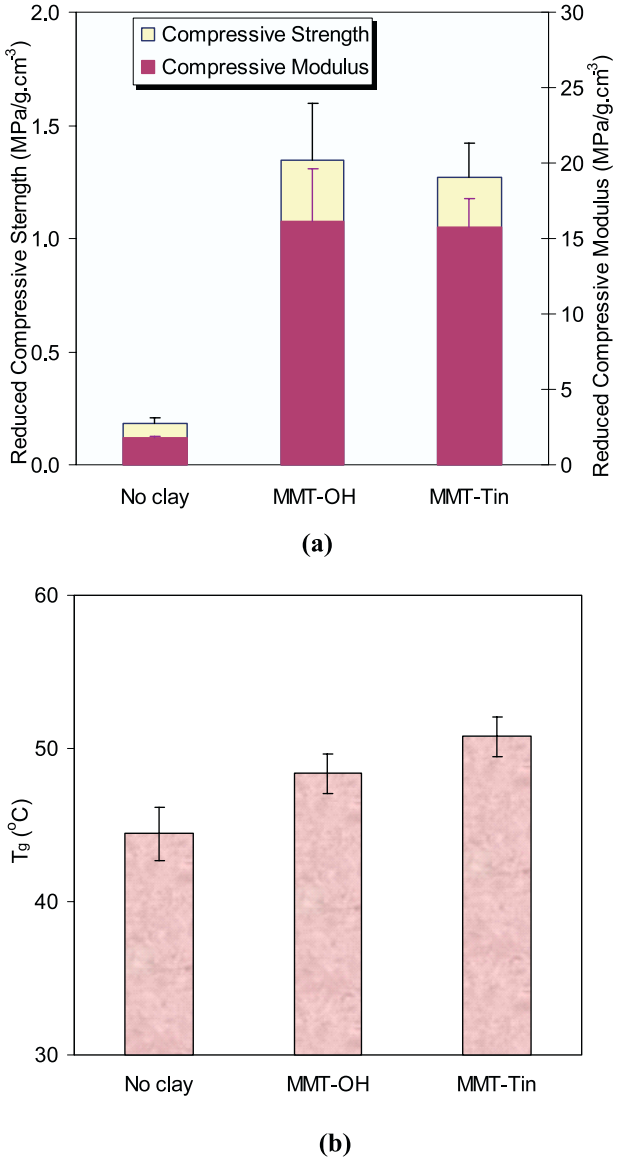

Fig. 9. Properties of 5 wt% clay/PU nanocomposite foams (a) compressive properties (b) glass transition temperature (polyol: Tone 0305).

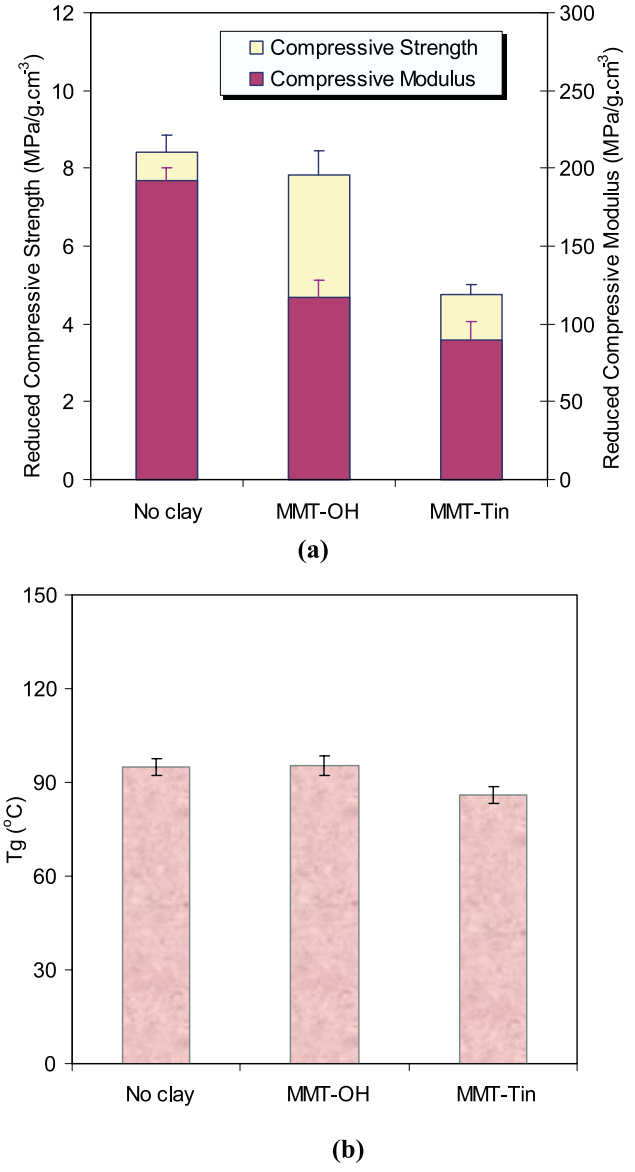

Fig. 10. Properties of 5 wt% clay/PU nanocomposite foams (a) compressive properties (b) glass transition temperature (polyol: Tone 0301).

PU foams prepared by Tone 0301, the urethane content is 0.87 mol/100 g, while the urethane content is only 0.65 mol/100 g for the foams prepared by Tone 0305. The overall performance of PU nanocomposite foams depends on the competition between the positive effects of clay on polymer reinforcement and foam morphology, and the negative effects on H-bond formation and network structure. The positive effects are stronger for the less rigid Tone 0305 foams, while the negative effects dominate for the more rigid Tone 0301 foams.

4. Conclusions

PU/organoclay nanocomposites were synthesized with montmorillonite clay containing different functional groups on the clay surface. Three methods based on in-situ polymerization were applied to prepare polyurethane nanocomposites. Premixing the functional clays with isocyanate provides better clay dispersion. Exfoliated structure can be achieved with clay bearing hydroxyl functional groups and intra-gallery organotin catalyst.

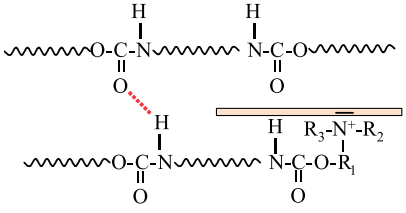

Fig. 11. The interference of grafted clay on H-bond formation in polyurethane.

The preparation and characterization of PU nanocomposite foams were also described in this study. Clay dispersion is affect by foaming process. With the inclusion of 5% functional organoclays, nanocomposite foams show a higher cell density with a smaller cell size. Depending on the chemical structure of polyurethane, as high as 650% increase in reduced compressive strength were observed in PU nanocomposite foam with relative low crosslinking density and urethane content but opposite effect was observed in PU nanocomposite foams with highly crosslinked structure and high urethane content.

Similar to our previous work on thermoplastic nanocomposite foams, nanocaly could lead to smaller cell size, higher cell density, and enhanced mechanical properties for thermoset polyurethane foams. However, unlike the thermoplastic nanocomposite foams in which better clay dispersion provides smaller cell size and higher cell density [9,10,16,17], better nanoparticle dispersion did not affect the cell morphology. Reactive foaming of polyurethane nanocomposites is a complicated process where many factors could influence bubble nucleation, bubble growth and coalescence, and in turn the cell morphology. Detailed mechanism on how nanoparticles influence cell morphology in reactive foaming needs further investigation.

Acknowledgements

The authors would like to thank Bayer Groups, Dow Chemical and Air Products and Chemicals for providing materials, and the NSF Center for Advanced Polymer and Composite Engineering (CAPCE) at The Ohio State University and the Industrial Partnership for Research in Interfacial and Materials Engineering (IPRIME) at the University of Minnesota for financial support. Valuable discussion and formulation suggestion from BASF are greatly appreciated.

References

[1] Giannelis EP. Advan Mater (Weinheim, Germany) 1996;8(1):29.
[2] Alexandre M, Dubois P. Mater Sci Eng, R: Rep 2000;R28(1–2):1.
[3] Giannelis EP, Krishnamoorti R, Manias E. Adv Polym Sci 1999;138:107.
[4] Wang Z, Pinnavaia TJ. Chem Mater 1998;10(12):3769.
[5] Chang JH, An YU. J Polym Sci, Part B: Polym Phys 2002;40(7):670.
[6] Tien YI, Wei KH. Macromolecules 2001;34(26):9045.
[7] Chen TK, Tien YI, Wei K-H. Polymer 2000;41(4):1345.
[8] Khemani KC. Polymeric foams: an overview. In: Khemani KC, editor. Polymeric foams: science and technology. Washington DC: American Chemical Society; 1997.
[9] Han X, Zeng C, Lee LJ, Koelling KW, Tomasko DL. Polym Eng Sci 2003;43(6):1261.
[10] Zeng C, Han X, Lee LJ, Koelling KW, Tomasko DL. Adv Mater (Weinheim, Germany) 2003;15(20):1743.
[11] Kresta JE, Wu JH, Crooker RM. In *Eur Pat Appl* 2002, (Atofina Chemicals, Inc., USA). EP 1209189 A1.
[12] Lepoittevin B, Pantoustier N, Devalckenaere M, Alexandre M, Kubies D, Calberg C, Jerome R, Dubois P. Macromolecules 2002;35(22):8385.
[13] Yang YS, Lee LJ. Macromolecules 1987;20(7):1490.
[14] Mitsunaga M, Ito Y, Ray SS, Okamoto M, Hironaka K. Macromol Mater Eng 2003;285(7):543.
[15] Colton JS, Suh NP. Polym Eng Sci 1987;27(7):485.
[16] Zeng C, Yang Y, Han X, Lee LJ, and Tomasko DL. Annual Technical Conference—Society of Plastics Engineers 61st(Vol. 2); 2003. p. 1635.
[17] Han X, Zeng C, Lee LJ, Koelling KW, Tomasko DL. Annual Technical Conference—Society of Plastics Engineers 60th(Vol. 2); 2002. p. 1915.